bioRxiv preprint doi: https://doi.org/10.1101/611988; this version posted April 22, 2019. The copyright holder for this preprint (which was not certified by peer review) is the author/funder. All rights reserved. No reuse allowed without permission.

1

2 **Can immunosuppressed mice control oral infection by the opportunistic pathogen**

3 ***Encephalitozoon intestinalis*?**

4

5 ***Encephalitozoon intestinalis* infection in immunosuppressed mice**

6

7

8

9 Maria Lucia da Costa Moura[a], Anuska Marcelino Alvares-Saraiva[a], Elizabeth Cristina Pérez[a], José

10 Guilherme Xavier[a], Diva Denelle Spadacci-Morena[b], Carla Renata Serantoni Moysés[a], Paulo

11 Ricardo Dell'Armelina Rocha[a], Maria Anete Lallo[a*]

12

13

14 [a] Programa de Pós-Graduação em Patologia Ambiental e Experimental, Universidade Paulista

15 (UNIP), Rua José Maria Whitaker 290, CEP 04057–000, São Paulo, SP, Brasil

16

17 [b] Departamento de Fisiopatologia, Instituto Butantan, Av. Vital Brasil 1500, CEP 05503–900, São

18 Paulo, SP, Brasil

19

20 *Corresponding author: Maria Anete Lallo – maria.lallo@docente.unip.br or

21 anetelallo@hotmail.com

22

23

bioRxiv preprint doi: https://doi.org/10.1101/611988; this version posted April 22, 2019. The copyright holder for this preprint (which was not certified by peer review) is the author/funder. All rights reserved. No reuse allowed without permission.

24

25 **Abstract**

26 Intestinal mucosa (IM), or the outer surface of the intestine, serves at the primary site for the
27 interaction of various pathogens that cause infection via the oral route. Thus, IM is crucial for
28 developing an efficient adaptive immune response against pathogenic micro-organisms, thereby
29 preventing their colonization and subsequent infection. In the present study, we investigated the
30 immune response to *Encephalitozoon intestinalis*-caused infection in the IM and gut-associated
31 lymphoid tissue (GALT) in C57BL/6 female mice. To mimic an immunosuppressive condition, the
32 mice were treated with cyclophosphamide (Cy). Histopathology revealed lymphoplasmacytic
33 enteritis at 7 and 14 days-post-infection (dpi) in all infected groups; however, inflammation
34 diminished at 21 and 28 dpi. Cy treatment also led to a higher number of *E. intestinalis* spores and
35 lesions, which reduced at 28 dpi. In addition, flow cytometry analysis demonstrated $CD4^+$ and
36 $CD8^+$ T cells to be predominant immune cells, with a significant increase in both Th1 and Th2
37 cytokines at 7 and 14 dpi, as demonstrated by histopathology. In conclusion, Cy treatment reduced
38 GALT (Peyer's plaques and mesenteric lymph nodes) and peritoneum populations but increased the
39 T-cell population in the intestinal mucosa and the production of pro-inflammatory cytokines, which
40 were able to eliminate this opportunistic fungus and reduced the infection.

41

42 **Keywords:** *Encephalitozoon intestinalis*, microsporidia, mucosal immunity, intestinal inflammation

43

44 **Introduction**

45 Microsporidia are spore-forming intracellular pathogens, responsible for causing opportunistic
46 infections in immunocompromised people, such as those with HIV infection and AIDS, cancer
47 patients or individuals with autoimmune diseases taking immunosuppressive drugs, and in elderly
48 and children (1-4). Two species are responsible for gastrointestinal infections: *Enterocytozoon*

bioRxiv preprint doi: https://doi.org/10.1101/611988; this version posted April 22, 2019. The copyright holder for this preprint (which was not certified by peer review) is the author/funder. All rights reserved. No reuse allowed without permission.

49 *bieneusi* and *Encephalitozoon intestinalis* (5). Both microsporidia are transmitted by the oral route
50 and cause abdominal cramping, diarrhea, malabsorption, and weight loss in patients with AIDS (6).
51 *E. intestinalis* also infects and develops inside intestinal macrophages, allowing the infection to
52 spread from the intestine to other organs (7). A very limited number of drugs are available for
53 treating intestinal microsporidiosis; these include albendazole and fumagillin, which are at least
54 partially effective in reducing the parasite count (2,7). A strong immune response of an individual is
55 mainly responsible for controlling the pathogen. The compartmentalized response against *E.*
56 *intestinalis* infection is primarily mediated by $CD8^{+}$ and $CD4^{+}$ T cells together with interferon
57 (IFN) and interleukin (IL)-12 cytokines (8,9).
58 The intestinal mucosa (IM) acts as a host to a variable microflora, which plays an important role in
59 nutrition absorption and immune function, among others. The immune response of the IM plays a
60 critical role in maintaining the commensal homeostasis and protecting the host against pathogens
61 (10,11). The immune response of IM against *E. cuniculi* infection is majorly mediated by antigen-
62 specific intraepithelial lymphocytes (IELs) (12). Considering the entry point of microsporidia to be
63 intestinal mucosa, there is a lack of knowledge of local immunity, especially in individuals on
64 immunosuppressive medications.
65 The past decade has witnessed a surge in the use of immunosuppressive drugs for the treatment of
66 neoplastic and autoimmune disease patients, as well as in patients undergoing transplantation.
67 Cyclophosphamide (Cy) is one such immunosuppressive drug that has been recommended by the
68 World Health Organization (WHO) and is on the list of drugs most frequently used by the Public
69 and Private Health Systems owing to its efficacy, cost-effectiveness, and lesser side-effects than
70 other drugs with similar actions, such as dexamethasone (13). Cy is primarily used against
71 autoimmune and alloimmune diseases (14,15), in treating patients undergoing transplantation, such
72 as bone marrow recipients (16) and in cancer treatment (17,18).
73 Cyclophosphamide is a cytotoxic alkylating agent that binds to DNA; its major effects on the body
74 include cellular apoptosis and myelosuppression, and decreased lymphocyte, neutrophil, red blood

bioRxiv preprint doi: https://doi.org/10.1101/611988; this version posted April 22, 2019. The copyright holder for this preprint (which was not certified by peer review) is the author/funder. All rights reserved. No reuse allowed without permission.

75 cell, and platelet count. However, it also possesses immunomodulatory effects, which have not yet
76 been clarified, such as (i) expansion of antigen-specific T cells, (ii) expansion of T cell-specific
77 cytokines (IFNs, IL-7, and IL-15), (iii) decrease in regulatory T cells (Treg), and (iv) increased
78 mobilization of dendritic cells from bone marrow, with activation of intracellular machinery for
79 antigen processing and presentation (19). Thus, this anticancer agent is known for inducing
80 immunogenic cancer cell death, subverting immunosuppressive T cells, and promoting Th1 and
81 Th17 cells that control cancer outgrowth (20, 21).
82 We have shown previously Cy to suppress the immune system of mice; intraperitoneal infection of
83 mice with *E. cuniculi* resulted in a disseminated, acute, and fatal encephalitozoonosis. These results
84 were associated with the immunosuppressive effects of Cy (22). This study was designed to
85 describe how the immunosuppressive effects of cyclophosphamide compromise the intestinal
86 immune response against *E. intestinalis*, one of the most prevalent microsporidia in opportunistic
87 infections in humans. Herein, we show a higher number of $CD8^+$ and $CD4^+$ T lymphocytes in IM in
88 association with pro-inflammatory cytokines to be responsible for resolution of *E. intestinalis*
89 infection in both Cy immunosuppressed and immunocompetent mice, despite the
90 immunosuppressive activity of Cy observed in cells populations of Peyer's plaques, mesenteric
91 lymph nodes, peritoneum and even part of the immune population of the IM.
92
93 **Results**
94 **Immunosuppressed mice showed transitory enteritis with fast resolution.** All infected mice
95 survived the oral infection by *E. intestinalis*, with no evidence of symptoms and macroscopic
96 lesions in the gut. Microscopically, lymphoplasmacytic enteritis was observed in infected animals
97 (*infected* and *Cy-infected)*, mostly affecting the duodenum and ileum, especially at 7 and 14 dpi
98 (Fig. 1a, b). In addition to the inflammatory infiltrate, mucosal ulceration caused exposure of the
99 underlying lamina propria (Fig. 1b), apical and mural multifocal necrosis, and villus-based
100 epithelial proliferation. At 21 and 28 dpi, young cells and an increased number of mitoses were

bioRxiv preprint doi: https://doi.org/10.1101/611988; this version posted April 22, 2019. The copyright holder for this preprint (which was not certified by peer review) is the author/funder. All rights reserved. No reuse allowed without permission.

101 observed in the small intestine, suggesting a restoration of tissue integrity, via resolution of the
102 inflammatory process and tissue remodeling. *E. intestinalis* spore clusters were observed on the
103 glandular base (Fig.1c), with a higher fungal burden observed in the *Cy-infected* than the *infected*
104 (Fig. 1d) group. However, in both groups, the fungal burden and the lesions progressively decreased
105 from 7 to 28 dpi (Fig. 1d). No *E. intestinalis* spores were observed in uninfected mice. Thus,
106 infection by *E. intestinalis* via oral route caused lymphoplasmacytic enteritis, accompanied by
107 favorable proliferation in both immunosuppressed and non-immunosuppressed groups; however,
108 the fungal burden was higher in the Cy-treated mice. Macroscopically, the infection led to the
109 enlargement of the spleen and intestinal lymph nodes in the infected animals.
110
111 **$CD8^+$ T lymphocytes increased in intestinal mucosa in infected mice.** The *infected* and *Cy-*
112 *infected* groups showed a significant increase in $CD8^+$ T lymphocyte population as compared to
113 controls at 7, 14, and 28 dpi (Fig. 2). This is in line with a previous study that demonstrated $CD4^+$ T
114 and $CD8^+$ T lymphocyte subpopulations to play a substantive role in protecting against peroral
115 infection of *E. intestinalis* (8). Another study reported a significant increase in the CD8αα subset of
116 IELs in response to oral *E. cuniculi* infection (12).
117 Immunosuppressive therapy with Cy could not cause a significant difference in $CD8^+$ T lymphocyte
118 population among the infected mice. Moreover, $CD8^+$ T lymphocyte population witnessed a 10-
119 time decrease, when compared 7 with 28 dpi (Supplementary Fig. 1). Together, the results showed
120 that $CD8^+$ T lymphocyte peak was observed at 7 dpi and was associated with a high number of *E.*
121 *intestinalis* spores and lymphoplasmacytic enteritis. At the same time, there was a gradual reduction
122 in the $CD8^+$ T cell population, fungal burden, and histological lesions in infected (*infected* and *Cy-*
123 *infected*) animals at 14, 21, and 28 dpi, indicating the resolution of infection in both
124 immunosuppressed and non-immunosuppressed groups. The treatment with Cy resulted in a
125 significant increase in the $CD4^+$ T lymphocyte population in the uninfected group. In addition,
126 *infected* and *Cy-infected* groups also showed an increase in this population at 14 and 28 dpi as

bioRxiv preprint doi: https://doi.org/10.1101/611988; this version posted April 22, 2019. The copyright holder for this preprint (which was not certified by peer review) is the author/funder. All rights reserved. No reuse allowed without permission.

127 compared to the untreated control (Fig. 2), suggesting that *E. intestinalis* stimulated $CD4^{+}$ T
128 expansion.
129 Further, the NKT cells decreased significantly in the *infected*, *Cy-infected,* and *Cy-uninfected*
130 groups as compared to the *uninfected* control at 7 and 14 dpi (Fig. 2). However, these cells
131 increased in the *infected* and *Cy-infected* groups in the later stages of infection (Supplementary 1).
132 A significant reduction in B-1 cells was reported in the *infected*, *Cy-infected*, and *Cy-uninfected*
133 groups as compared to the *uninfected* control at 14, 21, and 28 dpi (Fig. 2). Moreover, B-2 cells
134 decreased in the *infected* and *Cy-infected* groups as compared to the *uninfected* control at 14 dpi but
135 increased significantly in the *infected* group at 28 dpi (Fig. 2). Another notable observation was a
136 decrease in the dendritic cells in PP in the *infected* and *Cy-infected* groups (Fig. 3a). PP in the
137 *infected* group was more evident, with a marked increase in the germinal center activity, thereby
138 expanding the lymphoid center (Fig. 3b). Moreover, PP from *Cy-infected* mice showed a rarified
139 lymphoid tissue (Fig. 3b), enlarged lymphatics, and clusters of *E. intestinalis* spores (data not
140 shown).
141 Interestingly, Cy treatment (*Cy-uninfected*) showed an immunomodulatory effect on lymphocyte
142 populations in the intestinal mucosa. Overall, elevated levels of $CD8^{+}$ T, $CD4^{+}$ T, and B-2 cell
143 populations were observed as compared to other groups (Fig. 2).
144
145 **T and B lymphocytes decreased in mesenteric lymph nodes of *Cy-infected* mice.** The
146 populations of B-2, $CD4^{+}$ T, $CD8^{+}$ T, and NKT cells decreased at 21 and 28 dpi in the *Cy-infected*
147 group as compared to the *infected* group, suggesting the immunosuppressive effect of Cy. At 14 dpi,
148 a higher percentage of macrophages was present in the *Cy-infected* group as compared to the
149 *infected* group; however, this witnessed a decrease at 21 and 28 dpi (Fig. 4).
150
151 **T and B lymphocytes decreased in the peritoneum of *E. intestinalis*-infected mice.** The $CD4^{+}$ T,
152 $CD8^{+}$ T, and NKT cells decreased significantly in all *infected* groups as compared to the *uninfected*

bioRxiv preprint doi: https://doi.org/10.1101/611988; this version posted April 22, 2019. The copyright holder for this preprint (which was not certified by peer review) is the author/funder. All rights reserved. No reuse allowed without permission.

153 control (Fig. 5). Moreover, $CD8^+$ T, B-1, and B-2 lymphocytes decreased significantly in all Cy-
154 treated groups at 7 and 28 dpi (Fig. 5). At 14 dpi, both B-1 and B-2 cell populations and
155 macrophages increased in the *infected* group as compared to the *Cy-infected* group (Fig. 5).
156 However, the macrophage number decreased in the *infected*, *Cy-infected*, and *Cy-uninfected* groups
157 at 14 and 28 dpi (Fig. 5). Overall, the infected mice showed a decreased number of B-1, B-2, $CD4^+$
158 T, and $CD8^+$ T cells, with a statistical difference at 14 dpi (Supplementary Fig. 2). This difference
159 was maintained at 21 and 28 dpi for B cells, but not for T cells.
160
161 **Pro- and anti-inflammatory cytokines detected in the ileum of infected mice.** *E. intestinalis*
162 infection was associated with increased levels of various pro- and inflammatory cytokines,
163 including IL-10, IL-17a, TNF-α, IFN-γ, IL-6, IL-4, and IL-2 at 14 dpi (Fig. 6). High levels of TNF-
164 α persisted at 21 and 28 dpi, whereas other cytokines were not detected at these dpi (Fig. 6).
165 These results implied that Cy treatment increased the production of IL-10 and IFN-γ at 7 dpi in the
166 *Cy-uninfected* group as compared to the *uninfected* group. The highest level of cytokines was
167 observed in the *Cy-infected* mice and included mostly IL-2, IL-6 and IL-4. The cytokine IL-17a was
168 detected in all groups in all experimental animals although no statistical difference was observed
169 between them. Moreover, the *uninfected* group showed enhanced levels of TNF-α (Fig. 6).
170 Overall, the cytokines levels in the present study after *E. intestinalis* infection corroborate with the
171 histopathological results obtained in all *infected* groups at 7 and 14 dpi, reflecting the immune
172 system-mediated attempt to counter the intestinal infection.
173
174 **Transmission electron microscopy.** Transmission electron microscopy (TEM) results showed *E.*
175 *intestinalis* spores of varying shapes, from oval to piriform, to be present close to the
176 microvillosities and in the cytoplasm of enterocytes (Fig. 7) of the *Cy-infected* group. Additionally,
177 two patterns of the morphological invasion were observed: endocytosis (Fig. 7 a,b) and injection of
178 sporoplasm by polar tubule into the host cells (Fig. 7 c,d). The discontinuous microvillosities,

bioRxiv preprint doi: https://doi.org/10.1101/611988; this version posted April 22, 2019. The copyright holder for this preprint (which was not certified by peer review) is the author/funder. All rights reserved. No reuse allowed without permission.

179 present next to spores, showed invaginations, manifesting their attempt to engulf spores, a
180 mechanism similar to phagocytosis. However, no phagocytic vacuoles were observed (Fig. 7 a,b,c).
181 The cytoplasm surrounding the spores was found to be electrodense with a high number of
182 mitochondria (Fig. 7 a,b,c). Moreover, surrounding the *E. intestinalis* sporoplasm injection
183 demonstrated a loss of microvillosities and cytoplasmic membrane projections involving the
184 extruded polar tubule that appeared to form a channel for its entry into the electrodense cytoplasm
185 (Fig. 7 d).
186
187 **Discussion**
188 *E. intestinalis* invades and develops in the cytoplasm of enterocytes, causing persistent diarrhea in
189 humans with AIDS (7) or in individuals immunocompromised by cancer or chemotherapy (23,24).
190 Microsporidia also infect the macrophages of the lamina propria that help in its dissemination to
191 kidneys and the hepatobiliary tract (25). In the present study, we observed oral infection with *E.*
192 *intestinalis* not to be associated with clinical signs, such as diarrhea, even in the Cy-
193 immunosuppressed mice. However, microscopically, lymphoplasmacytic enteritis was observed in
194 association with *E. intestinalis* spores.
195 The adaptive immune response is very crucial for containing microsporidiosis. For example, T
196 cells-deficient mice (athymic/nude or SCID) are incapable of successfully killing the pathogen and
197 die due to encephalitozoonosis as opposed to immunocompetent mice (1,26). Similarly, IFN-$\gamma^{-/-}$
198 mice lacking major proinflammatory cytokines showed hepatomegaly, colicystitis, splenomegaly,
199 intestinal enlargement, and ascites three to four weeks post infection with *E. intestinalis*. Moreover,
200 these mice could live only up to six weeks post infection (25). Therefore, physical or genetic
201 deletion of immune cells or cytokines represents a situation that does not correspond to clinical
202 observations observed in individuals immunosuppressed by drugs. Since immunosuppressive drugs
203 act on different cells of the immune system, leading to a diversity of immunocompromised states,
204 we used Cy to mimic the physiological immunosuppression situations.

bioRxiv preprint doi: https://doi.org/10.1101/611988; this version posted April 22, 2019. The copyright holder for this preprint (which was not certified by peer review) is the author/funder. All rights reserved. No reuse allowed without permission.

205 We observed that *Cy-infected* mice showed a higher number of spores, reflecting the increased
206 susceptibility to pathogen upon treatment with Cy, as previously reported by our group in
207 experimental *E. cuniculi* infection in mice (22). Unexpectedly, the present results showed a
208 decrease in fungal burden and histopathological lesions in immunosuppressed mice at 21 and 28
209 dpi, indicating successful elimination of pathogen. Cy treatment is lymphotoxic and rapidly
210 decreases the T and B cell populations (14). However, a study reported it to cause an extensive
211 mobilization of immune cells from the bone marrow and other lymphoid organs (18). In the present
212 study, we observed an increase in $CD4^+$ T and $CD8^+$ T cells population in the IM of Cy-treated
213 mice. These results may be associated to two possible explanations: i) the displacement of immune
214 cells from nearby immune sites such as Peyer's patches, lymph nodes and peritoneum favored the
215 assembly of an immune response in the gut capable of controlling infection, however, in this case, it
216 should be considered that such reduction could be linked to the suppressive effect of Cy on these
217 immune sites, or ii) low action on the immune population of the intestinal mucosa, especially T
218 cells, data that may be linked to a possible immunomodulatory activity of Cy, which should be
219 further explored
220 Another observation that point toward resolution of infection is the increased presence of mitosis in
221 the intestinal crypts of the small intestine associated with enteritis in all infected animals, indicating
222 tissue remodeling in the intestine under both pathological and physiological conditions (27). Since
223 enterocytes serve as the first physical barrier against pathogens in intestine, maintenance of a strong
224 epithelial barrier is crucial for normal physiology and evasion of infections. Moreover, epithelial
225 cells secrete important chemoattractants that are involved in cell chemotaxis (28). The IELs
226 constitute a sub-population of T lymphocytes in the IM that has been implicated in both intestinal
227 homeostasis and inflammation, as observed in intestinal toxoplasmosis. Another important category
228 of immune cells is dendritic cells that reside in the lamina propria beneath the IM and act as antigen
229 presenting cells. They play a crucial role in containing toxoplasmosis. Lamina propria also

bioRxiv preprint doi: https://doi.org/10.1101/611988; this version posted April 22, 2019. The copyright holder for this preprint (which was not certified by peer review) is the author/funder. All rights reserved. No reuse allowed without permission.

230 comprises $CD4^+$ T, $CD8^+$ T, and B lymphocytes; B cells are known for producing secretory IgA
231 that is responsible for the exclusion of environmental antigens (29).
232 There are reports stating an effective immune response against microsporidia to involve majorly
233 $CD8^+$ T cells (30,31). Interestingly, other studies report $CD8^+$ T cells and not $CD4^+$ T cells to be
234 indispensable in successfully eliminating pathogens in intraperitoneal infection by *E. cuniculi*
235 (30,32). In fact, the dichotomic role of $CD4^+$ T cells has been shown to be associated with the
236 infection route. It has been shown that the oral infection with *E. cuniculi* stimulates a synergistic
237 effect of $CD8^+$ and $CD4^+$ T cells (12). The present study also reported an increased number of $CD4^+$
238 T cells in the intestines of infected mice, contributing to successful *E. intestinalis* elimination. We
239 believe this increase in $CD4^+$ T cells to be attributed to the immunomodulatory effect of Cy in the
240 intestinal mucosa.
241 Evidence from literature reports $CD4^+$ and $CD8^+$ T cells, associated with IFN-γ and IL-12
242 cytokines, to be important players in eliminating *E. intestinalis* infection (8,9). The present results
243 reinforce this hypothesis; as evident by a significant increase in $CD8^+$ T cells in all infected groups.
244 A subsequent decrease in $CD8^+$ T cell population was associated with a decrease in spore numbers
245 and histopathological lesions. At 7 and 14 dpi, the increased production of TNF-α, IFN-γ, and IL-10
246 cytokines was noticed in the ileum of infected mice, together with an increase in IL-2 and IL-4 in
247 *Cy-infected* mice. The results suggest that besides IFN-γ (8,9), other cytokines, including anti-
248 inflammatory cytokines, play a crucial role in mediating an intestinal immune response against *E.*
249 *intestinalis*, for the resolution of enteritis and pathogen killing.
250 The IELs comprise a heterogeneous population, predominantly composed of $CD8^+$ T (CD8αα and
251 CD8αβ) cells and a few $CD4^+$ T lymphocytes and known to play an important role in oral
252 infections. Upon infection, an expansion in the number of these cells causes increased production of
253 IFN-γ, cytolytic properties of which inhibit intestinal *E. cuniculi* proliferation and dissemination
254 (12). In fact, our results showed an increased $CD8^+$ T IELs in intestinal *E. intestinalis* infection.
255 However, $CD8^+$ T cells decreased in the peritoneal cavity, suggesting their migration to the site of

bioRxiv preprint doi: https://doi.org/10.1101/611988; this version posted April 22, 2019. The copyright holder for this preprint (which was not certified by peer review) is the author/funder. All rights reserved. No reuse allowed without permission.

256 pathogen proliferation. This finding is in corroboration to previous studies that have already shown
257 cells in the peritoneal cavity to migrate to other sites (33,34).
258 Our group has previously shown B-1 cells to be an important player in the generation of the
259 immune response against *E. cuniculi* infection (35,36). B-1 cells are important in generating
260 adaptive immune response and antibody production, which is independent of T cells (37). However,
261 B-1 cells are also dependent on T cells for generating an effective immune response, such as cell-
262 mediated hypersensitivity (38,39) and rejection of aloenxerts (40). Moreover, adoptive transfer of
263 B-1 cells activates T cells that produce IFN-γ (41). Here, we showed a decrease in B-1 cell
264 frequency in *infected* animals as compared to controls of both intestine and peritoneal cavity. We
265 hypothesized that B-1 cells from the peritoneal cavity differentiated into B-1 cell-derived phagocyte
266 (B-1 CDP) in infected mice, which, in turn, promoted phagocytosis of *E. intestinalis* spores. *In vitro*
267 studies showed that B-1 cells may also differentiate into mononuclear phagocytes, which upon
268 attachment to a substrate, acquire a myeloid phenotype (33). Moreover, *Propionibacterium acnes*
269 infection of B-1 cells of myeloid lineage induced only differentiation into phagocytes (42);
270 however, the role of B-1 cells in the intestines warrants further understanding of microsporidia
271 infection.
272 We also found a decrease in the NKT cells in the intestine and mesenteric lymph nodes in all
273 infected mice. NKT cells are known to play a protective role in *Toxoplasma gondii* oral infection
274 although these cells are susceptible to direct invasion by the parasite (43). In fact, NKT cells
275 develop a hypermotility phenotype *in vivo* during *T. gondii* oral infection, suggesting manipulation
276 of motility of immune cells by *T. gondii*, which assist in the spread of the causative organism
277 (44,45), as already shown in macrophages (45). *E. cuniculi* uses macrophages as a Trojan horse
278 (46); however, whether this phenomenon occurs with NKT cells in microsporidiosis remains largely
279 unknown.
280 While an effective immune response against microsporidia is predominantly driven by T cells,
281 dendritic cells have also been shown to play an important and critical role in stimulating these cells.

bioRxiv preprint doi: https://doi.org/10.1101/611988; this version posted April 22, 2019. The copyright holder for this preprint (which was not certified by peer review) is the author/funder. All rights reserved. No reuse allowed without permission.

282 Dendritic cells of the IM act as antigen-presenting cells and are responsible for priming T naive
283 cells in effectors and memory cells upon infection (47). The secretion of cytokines and chemokines
284 from infected enterocytes results in migration of these cells from PP to the mucosa (28). On the
285 other hand, a study reported *in vitro* inhibition of dendritic cell differentiation by *E. intestinalis*
286 (48). On the same lines, we, in the present study, demonstrate a reduction in dendritic cells in PP of
287 infected animals at 7 and 14 dpi, which was associated with a higher number of fungal spores and
288 histopathological lesions, suggesting the migration of these cells to the site of infection.
289 In the gastrointestinal tract, dendritic cells play an important role in suppression of colitis
290 development, inducing the traffic of T regulatory cells in the intestine, and inducing IgA secretion
291 from B cells in the intestine (28). These are also involved in inducing oral tolerance and preventing
292 inflammatory response mediated by gut microbiota and ingested antigens (28). The breach in this
293 function may decrease the number of T regulatory cells and increase the number of cells producing
294 *Th1* and *Th17* cytokines (28). A lower frequency of dendritic cells observed in the present study is
295 related to a higher parasite burden; however, this is yet to be clarified.
296 It has been previously shown that microsporidia spores infect new cells mostly by injection of
297 sporoplasm into the host cells via the polar tubule (49). However, different cell lineages are capable
298 of phagocytosing microsporidia spores (50,51), suggesting endocytosis to be an important
299 mechanism in intestinal microsporidiosis. In order to evade this protective mechanism,
300 microorganisms have developed complex systems to subvert endocytosis by host cells, allowing
301 invasion of even those cells that generally do not phagocytose (52). Previous studies have suggested
302 microsporidia to induce invaginations of the cell membrane of host cells close to the polar tubule in
303 a process similar to endocytosis, causing injection of sporoplasm into the host cell. The results of
304 TEM showed that a phenomenon similar to phagocytosis occur more frequently in *E. intestinalis*
305 infection.
306 The results of this study showed that the increase in the $CD8^+$ and $CD4^+$ T cell population in the
307 intestinal mucosa of Cy immunosuppressed mice and orally infected with *E. intestinalis*, in

bioRxiv preprint doi: https://doi.org/10.1101/611988; this version posted April 22, 2019. The copyright holder for this preprint (which was not certified by peer review) is the author/funder. All rights reserved. No reuse allowed without permission.

308 association with the presence of pro-inflammatory cytokines, controlled the infection by the
309 opportunistic fungus, although reduction of cellular populations at immune sites has been observed,
310 confirming a state of immunosuppression, reinforcing that the selective effect of Cy should be
311 better understood.
312
313 **Methods**
314 **Animals**
315 Specific pathogen-free, 6–8-week-old C57BL/6 mice were purchased from the Federal University
316 of São Paulo (CEDEME, UNIFESP), Brazil. Animals were housed under sterile conditions at the
317 Animal Facility of Paulista University, São Paulo, Brazil, and given food and water *ad libitum*. All
318 animal procedures were performed in strict accordance with the Paulista University Ethics
319 Committee (project license no. 313/15).
320
321 ***Encephalitozoon intestinalis* cultivation and experimental infection**
322 Spores of *E. intestinalis* were purchased from Waterborne Inc., New Orleans, LA, United States.
323 These were cultivated in rabbit kidney cells (RK–13) in Dulbecco's Modified Eagle's medium
324 (DMEM) supplemented with 10% fetal bovine serum (FBS), pyruvate, non-essential amino acids,
325 and gentamicin followed by incubation at 37 °C and 5% CO_2. Spores were collected from the
326 supernatant, washed thrice in phosphate-buffered saline (PBS), and counted using a Neubauer
327 chamber.
328
329 **Study design**
330 Mice were divided into four experimental groups: *infected*, mice infected with *E. intestinalis*;
331 *uninfected*, non-infected and non-treated mice; *Cy-infected*, mice treated with cyclophosphamide
332 and infected with *E. intestinalis*; and *Cy-uninfected*, mice treated with cyclophosphamide. The Cy-
333 treatment protocol was previously established (22) and consisted of intraperitoneal injection of 100

bioRxiv preprint doi: https://doi.org/10.1101/611988; this version posted April 22, 2019. The copyright holder for this preprint (which was not certified by peer review) is the author/funder. All rights reserved. No reuse allowed without permission.

334 mg/kg twice a week (Genuxal; Asta Medica Oncologia, São Paulo, Brazil). The treatment started at
335 the day of infection until 28 days post infection (dpi). Mice were orally infected by gavage with 5×
336 10^7 *E. intestinalis* spores. Non-infected mice served as control.
337
338 **Necropsy and tissue sampling**
339 At 7, 14, 21, and 28 dpi, five animals from each group were euthanized with a mixture of ketamine
340 (100 mg/mL), xylazine (20 mg/mL), and fentanyl (0.05 mg/mL). The samples of the intestine
341 (duodenum, ileum), liver, kidneys, and lungs were collected and fixed in 10% buffered formalin for
342 72 h, routinely processed for histopathology, and stained with hematoxylin-eosin (HE) and Giemsa.
343
344 **Ultrastructural analysis by transmission electronic microscopy**
345 Ileum samples of 1 mm thickness from Cy-infected mice were fixed in 2% glutaraldehyde in 0.2 M
346 cacodylate buffer (pH 7.2) at 4 °C for 10 h. These were then fixed in buffered 1% OsO4 for 3 h.
347 Subsequently, the samples were embedded in EPON resin, sliced into semi-thin cuts, and stained
348 with toluidine blue. Then, ultrathin sections were double stained using uranyl and lead citrate and
349 observed under the TEM LEO EM 906 at 80 kV at the Butantan Institute.
350
351 **Fungal burden**
352 The paraffinized ileum was cut into 5-µm thick sections and evaluated histopathologically using HE
353 staining to determine the fungal number. Fungal spores were counted randomly in at least 10 fields
354 under the light microscope (40× objective magnification). The average number of spores from each
355 mice was recorded and statistically analyzed.
356
357 **Phenotypic analysis of immune intestinal mucosal cells**
358 Cells of the IM were obtained as previously described,[53] with minor modifications. The small
359 intestine was washed with 50 mL of Hanks' balanced salt solution (HBSS)–2% FBS solution,

bioRxiv preprint doi: https://doi.org/10.1101/611988; this version posted April 22, 2019. The copyright holder for this preprint (which was not certified by peer review) is the author/funder. All rights reserved. No reuse allowed without permission.

360 longitudinally cut and separated into 2-cm segments. The mucosa was grated and submerged in
361 HBSS–2% FBS solution supplemented with 0.1 M ethylenediaminetetraacetic acid (EDTA) at 37°C
362 for 20 min. Then, samples were vortexed for 15 s and filtered using a cell strainer to remove the cell
363 debris. Percoll gradient (70% and 40%) centrifugation was used to isolate the IM cells. After
364 centrifugation, cells were washed with HBSS–2% FBS and resuspended in 100 μL of PBS–1%
365 bovine serum albumin (BSA).
366 Mesenteric lymph nodes (MLN) and Peyer's patches (PP) were isolated from the intestines using a
367 scalped blade and washed in a cell strainer with HBSS–2% FBS. In addition, cells from the
368 peritoneal cavity (PerC) were obtained by successive washes with at least 10 mL of HBSS–2%
369 FBS. Finally, cell suspensions from PerC, MLN, and IM were washed with HBSS–2% FBS and
370 resuspended in 100 μL of PBS–1%BSA. After centrifugation at 500 ×g for 5 min, each sample was
371 incubated at 4 °C for 20 min with the anti-CD16/CD32 antibody. After incubation, cells were
372 divided into two aliquots and resuspended in PBS–1%BSA, followed by incubation with
373 monoclonal antibodies: APC-conjugated anti-mouse CD19, FITC, or PE-conjugated anti-mouse
374 CD23, PerCP-conjugated anti-mouse CD4, FITC-conjugated anti-mouse CD8, APC-Cy7-
375 conjugated anti-mouse CD11b, and PE-conjugated anti-mice CD11c (BD Pharmingen; San Diego,
376 CA, United States). Finally, cell suspensions were run on the flow cytometer FACS Canto II (BD
377 Biosciences; Mountain View, CA, United States). The cells were characterized according to their
378 phenotypes in CD8 T ($CD19^{-}$ $CD4^{-}$$CD8^{+}$), CD4 T ($CD19^{-}$ $CD8^{-}$ $CD4^{+}$), NKT cells ($CD19^{-}$ $CD4^{+}$
379 $NK1.1^{+}$), B-1 ($CD23^{-}$ $CD19^{+}$), B-2 cells ($CD23^{+}$ $CD19^{+}$) and dendritic cells ($CD11c^{+}$); and analyzed
380 with the software FlowJo (FlowJo LLC; data analysis software, Ashland, OR, United States).
381

382 **Cytokine quantification**

383 For quantification of intestinal cytokines, 100 mg of ileum was sampled and treated with 1 mL of
384 protease inhibitor (Sigma-Aldrich; St. Louis, MO, United States) at −80 °C. The sample was
385 thawed and processed using a Precellys homogenizer for three cycles, 20 s each, filtering the

bioRxiv preprint doi: https://doi.org/10.1101/611988; this version posted April 22, 2019. The copyright holder for this preprint (which was not certified by peer review) is the author/funder. All rights reserved. No reuse allowed without permission.

386 homogenate using a cell strainer to remove the debris. Cytokines (IL-2, IL-4, IL-6, IL-10, IL-17,
387 IFN-γ, and TNF-α) in the homogenate were measured using the CBA Mouse Th1/Th2/Th17
388 cytokine kit (BD Biosciences; CA, United States) according to manufacturer's instructions. The kit
389 consists of fluorescent beads coated with antibodies specific to cytokines. Briefly, 25 μL of each
390 sample was added to capture beads and PE-labeled secondary antibodies. The samples were
391 incubated for 2 h at room temperature in the dark, following which two-color flow cytometry
392 analysis was performed on the FACS Canto II flow cytometer (BD Biosciences; Mountain View,
393 CA, United States) and analyzed using the FCAP Array 1.0 software (BD Biosciences; CA, United
394 States).
395
396 **Statistical analysis**
397 Analysis of variance (ANOVA) tests and Tukey's or Bonferroni's multiple comparison post-tests
398 were used for the statistical analysis of data. All values are expressed as mean ±standard error mean
399 (SEM) with significance of $\alpha = 0.05$ ($p < 0.05$). All graphs were generated using the "GraphPad
400 Prism" version 5.0 for Windows (GraphPad Software Inc; La Jolla, CA, United States).
401
402 **Acknowledgments**

403 We thank Magna Maltauro Soares (Instituto Butantan) for histopathological processing. We thank
404 Fundação de Amparo à Ciência do Estado de São Paulo–Fapesp and Capes for financial support.
405
406 **Competing interests**

407 The authors declare no competing interests

408
409 **References**
410 1. Moretto M, Khan IA, Weiss LM. 2012. Gastrointestinal cell mediated immunity and the
411 microsporídia. Plos Pathogen 8: e.100 2765.

bioRxiv preprint doi: https://doi.org/10.1101/611988; this version posted April 22, 2019. The copyright holder for this preprint (which was not certified by peer review) is the author/funder. All rights reserved. No reuse allowed without permission.

412 2. Didier ES, Weiss LM. 2011. Microsporidiosis: not just in AIDS patients. Curr Opin Infect Dis
413 24:490–495.
414 3. Kicia M, Wesolowawska M, Jakuszko K, Kopacz Z, Sak B, Květonova D. Krajewska M, Kváč
415 M. 2014. Concurrent infection of the urinary tract with *Encephalitozoon cuniculi* and
416 *Enterocytozoo;n bieneusi* in a renal transplant recipient. J Clin Microbiol 52:1780–1782.
417 4. Hinney B, Sak B, Joachim A, Kváč M. 2016. More than a rabbit's tale e *Encephalitozoon* spp. in
418 wild mammals and birds. Int J Parasitol 5:76–87.
419 5. Field AS, Milner DA. 2015. Intestinal microsporidiosis. Clin Lab Med 35:445–459.
420 6. Han B, Weiss LM. 2017. Microsporidia: Obligate Intracellular Pathogens within the Fungal
421 Kingdom. Microbiol Spectr 5. doi:10.1128/microbiolspec. FUNK–0018–2016.
422 7. Didier ES. 2005. Microsporidiosis: an emerging and opportunistic infection in human and
423 animals. Acta Trop. 94:61–76.
424 8. Salát J, Sak B, Le T, Kopecký J. 2004. Susceptibility of IFN- gamma or IL-12 knock-out and
425 SCID mice to infection with two microsporidian species, *Encephalitozoon cuniculi* and *E.*
426 *intestinalis*. Folia Parasitol 51:275–282.
427 9. Salát J, Horká H, Sak B, Kopecký J. 2006. Pure $CD4^+$ T-lymphocytes fail to protect perorally
428 infected SCID mice from lethal microsporidiosis caused by *Encephalitozoon cuniculi*. Parasitol Res
429 99:682–686.
430 10. Allaire JM, Crowley SM, Law HT, Chang S, Ko H, Vallance BA. 2018. The intestinal
431 epithelium: central coordinator of mucosal immunity. Trends Immunol. 39:677-696.
432 https://doi.org/10.1016/j.it.2018.04.002.
433 11. Mangan NE, Fung,KY. 2012. Type I interferons in regulation of mucosal immunity. Immunol
434 Cell Biol 90:510–519.
435 12. Moretto M, Weiss LM, Khan IA. 2004. Induction of a rapid and strong antigen-specific
436 intraepithelial lymphocyte response during oral *Encephalitozoon cuniculi* infection. J Immunol
437 172:4402–4409.

bioRxiv preprint doi: https://doi.org/10.1101/611988; this version posted April 22, 2019. The copyright holder for this preprint (which was not certified by peer review) is the author/funder. All rights reserved. No reuse allowed without permission.

438 13. World Health Organization. 2013. WHO Model list of Essential Medicine.
439 http://www.who.int/medicines/publications/essentialmedicines/18th_EML.pdf.
440 14. Brodsky RA. 2010. High-dose cyclophosphamide for autoimmunity and alloimmunity.
441 Immunol Res 47:79–84.
442 15. Dezern AE, Styler MJ, Drachman DB, Hummers LK, Jones RJ, Brodsky RA. 2013. Repeated
443 treatment with high dose cyclophosphamide for severe autoimmune diseases. Am J Blood Res
444 3:84–90.
445 16. Colvin OM. 1999. An overview of cyclophosphamide development and clinical applications.
446 Curr Pharm Des 5:555–560.
447 17. Emadi AL, Jones RJ, Brodsky RA. 2009. Cyclophosphamide and cancer: golden anniversary.
448 Nat Rev Clin Oncol 6:638–647.
449 18. Sistigu A, Viaud S, Chaput N, Bracci L, Proietti E, Zitvogel L. 2011. Immunomodulatory
450 effects of cyclophosphamide and implementations for vaccine design. Semin Immunopathol
451 33:369–383.
452 19. Sevko A, Sade-Feldman M, Kanterman J, Michels T, Falk CS, Umnsky L, Ramacher M, Kato
453 M, Schadendorf D, Baniyash M, Umansky V. 2013. Cyclophosphamide promotes chronic
454 inflammation-dependent immunosuppression and prevents antitumor response in melanoma. J
455 Invest Dermatol 133:1610–1619.
456 20. Schiavoni G, Sistigu A, Valentini M, Mattei F, XSestili P, Spadaro F, Sanchez M, Lorenzi S,
457 D'Urso MT, Belardelli F, Gabriele L, Proietti E, Braccio L. 2011. Cyclophosphamide synergizes
458 with type I interferons through systemic dendritic cell reactivation and induction of immunogenic
459 tumor apoptosis. Cancer Res 71:768–778.
460 21. Viaud S, Flament C, Zoubir M, Pautier P, LeCesne A, Ribrag V, Soria JC, Marty V, Vielh P,
461 Robert C, Chaput N, Zitvogel L. 2011. Cyclophosphamide induces differentiation of Th17 cells in
462 cancer patients. Cancer Res. 71:661–665.

bioRxiv preprint doi: https://doi.org/10.1101/611988; this version posted April 22, 2019. The copyright holder for this preprint (which was not certified by peer review) is the author/funder. All rights reserved. No reuse allowed without permission.

463 22. Lallo MA, Hirschfeld MMP. 2012. Encephalitozoonosis in pharmacologically
464 immunosuppressed mice. Exp Parasitol 131:339–343.
465 23. Chabchoub N, Abdelmalek R, Mellouli F, Kanoun F, Thellier M, Bouratbine A, Aoun K. 2009.
466 Genetic identification of intestinal microsporidia species in immunocompromised patients in
467 Tunisia. Am J Trop Med Hyg 80:24–27.
468 24. Hamamci B, Çetinkaya Ü, Berk V, Kaynar L. 2015. Prevalence of *Encephalitozoon intestinalis*
469 and *Enterocytozoon bieneusi* in cancer patients under chemotherapy.
470 Mikrobiyol Bul 49:105–113.
471 25. El Fakhry Y, Achbarou A, Franetich JF, Desportes-Livage I, Mazier D. 2001. Dissemination of
472 *Encephalitozoon intestinalis*, a causative agent of human microsporidiosis, in IFN-gamma receptor
473 knockout mice. Parasite Immunol 23:19–25.
474 26. Gannon J. 1980. The course of infection of *Encephalitozoon cuniculi* in immunodeficient and
475 immunocompetent mice. Lab Anim 14:189–192.
476 27. Fuss IJ, Heller F, Boirivant M, Leon F, Yoshida M, Fichtner-Feigi S, Yang Z, Exley M, Kitani
477 A, Blumberg RS, Mannon P, Sttober W. 2004. Nonclassical CD1d-restricted NK T cells that
478 produce IL-13 characterize an atypical Th2 response in ulcerative colitis. J Clin Invest 15:1490–
479 1497.
480 28. Goodman WA, Pizarro TT. 2013. Regulatory cell populations in the intestinal mucosa. Curr
481 Opin Gastroenterol 29:614–620.
482 29. Cohen SB, Denkers EY. 2015. The gut mucosal immune response to *Toxoplasma gondii*.
483 Parasite Immunol 37:108–117.
484 30. Braunfuchsová P, Salát J, Kopecký J. 2001. $CD8^+$ T-lymphocytes protect SCID mice against
485 *Encephalitozoon cuniculi* infection. Int J Parasitol 15:681–686.
486 31. Khan IA, Schwartzmn JD, Kasper LH, Moretto M. 1999. $CD8^+$CTLS are essencial for
487 protective against *Encephalitozoon cuniculi* infection. J Immunol 162:6086–6091.

bioRxiv preprint doi: https://doi.org/10.1101/611988; this version posted April 22, 2019. The copyright holder for this preprint (which was not certified by peer review) is the author/funder. All rights reserved. No reuse allowed without permission.

488 32. Moretto M, Casciotti L, Durell B, Khan IA. 2000. Lack of $CD4^+$ T cells does not affect
489 induction of $CD8^+$ T-cell immunity against *Encephalitozoon cuniculi* infection. Infect Immun
490 68:6223–6232.
491 33. Almeida SR, Aroeira LS, Frymuller E, Dias MA, Bogsan CS, Lopes JD, Mariano M. 2001.
492 Mouse B-1 cell-derived mononuclear phagocyte, a novel cellular component of acute non-specific
493 inflammatory exudate. Int Immunol 13:1193–201.
494 34. Palos MC, Azevedo MC, Thies FG, Osugui L, Alveres AM, Laurindo MF, Russo RT, Popi AF,
495 Mariano M. 2012. Different inflammatory stimuli in the footpad of mice influence the kinetics of
496 resident peritoneal cells. Inflamm Res 61:1187–1194.
497 35. Da Costa LF, Alvares-Saraiva AM, Dell'Armelina Rocha PR, Spadacci-Morena DD, Perez EC,
498 Mariano M, Lallo MA. 2017. B-1 cell decreases susceptibility to encephalitozoonosis in mice.
499 Immunobiol 222:218–227.
500 36. Langanke dos Santos D, Alvares-Saraiva AM, Xavier, JG, Spadacci-Morena DD, Peres GB,
501 Dell'Armelina Rocha PR, Perez EC, Lallo MA. 2018. B-1 cells upregulate CD8 T lymphocytes and
502 increase proinflammatory cytokines serum levels in oral encephalitozoonosis. Microbes Infect
503 20:196–204.
504 37. Choi YS., Baumgarth N. 2008. Dual role for B-1a cells in immunity to influenza virus infection.
505 J Exp Med 205:3053–3064.
506 38. De Lorenzo B, Brito RR, Godoy LC, Lopes JD, Mariano M. 2007. Tolerogenic property of B-
507 1b cells in a model of allergic reaction. Immunol Lett 114:110–118.
508 39. Szczepanik M, Akahira-Azuma M, Bryniarski K, Tsuji RF, Kawikova I, Ptak W, Kiener C,
509 Campos RA, Askenase PW. 2003. B-1 B cells mediate required early T cell recruitment to elicit
510 protein-induced delayed-type hypersensitivity. J Immunol 171:6625–6635.
511 40. Nogueira-Martins MF, Mariano M. 2010. B-1 cell participation in T-cell-mediated alloimmune
512 response. Immunobiol 215,:264–274.

bioRxiv preprint doi: https://doi.org/10.1101/611988; this version posted April 22, 2019. The copyright holder for this preprint (which was not certified by peer review) is the author/funder. All rights reserved. No reuse allowed without permission.

513 41. Margry B, Wieland WH, van Kooten PJ, van Eden W, Broere F. 2013. Peritoneal cavity B-1a
514 cells promote peripheral CD4+ T-cell activation. Eur J Immunol 43:2317–2326.
515 42. Mussalem JS, Squaiella-Baptistão CC, Teixeira D, Yendo TM, Thies FG, Popi AF, Mariano M,
516 Longo-Mauregi I. 2012. Adjuvant effect of killed *Propionibacterium acnes* on mouse peritoneal B-
517 1 lymphocytes and their early phagocyte differentiation. Plos One 7: e33955.
518 doi:10.1371/journal.pone.0033955.
519 43. Persson CM, Lambert H, Vutova PP, Dellacasa-Lindberg I, Nederby J, Yagita H, Ljunggren
520 HG, Gradien A, Barragan A, Chambers BJ. 2009. Transmission of *Toxoplasma gondii* from
521 infected dendritic cells to natural killer cells. Infect Immun 77:970–976.
522 44. Harker KS, Ueno N, Wang T, Bonhomme C, Liu W, Lodoen MB. 2013. *Toxoplasma gondii*
523 modulates the dynamics of human monocyte adhesion to vascular endothelium under fluidic shear
524 stress. J Leukoc Biol 93:789–800.
525 45. Seipel D, Oliveira BC, Resende TL, Schuindt SH, Pimentel PM, Kanashiro MM, Amholdt AC.
526 2010. *Toxoplasma gondii* infection positively modulates the macrophages migratory molecular
527 complex by increasing matrix metalloproteinases, CD44 and alpha v beta 3 integrin. Vet Parasitol
528 169:312–319.
529 46. Mathews A, Hotard A, Hale-Donze H. 2009. Innate immune responses to *Encephalitozoon*
530 species infections. Microbes Infect. 11:905–911.
531 47. Steimnman RM, Hemmi H. 2006. Dendritic cells: translating innate to adaptive immunity. Curr
532 Top Microbiol Immunol 311:17–58.
533 48. Bernal JA, Andrés M, Palmero MF. 2016. Bruton´s tyrosine kinase inhibitors could induce
534 rheumatoid arthritis-like manifestations: A comment on the article by Nyhoff et al. Arthritis
535 Rheumatol 16:475.
536 49. Leitch GJ, Ward TL, Shaw AP, Newman G. 2005. Apical spore phagocytosis is not a significant
537 route of infection of differentiated enterocytes by *Encephalitozoon intestinalis*. Infect Immun
538 73:7697–7704.

bioRxiv preprint doi: https://doi.org/10.1101/611988; this version posted April 22, 2019. The copyright holder for this preprint (which was not certified by peer review) is the author/funder. All rights reserved. No reuse allowed without permission.

539 50. Couzinet S, Cejas E, Schittny J, Deplazes P, Weber R, Zimmerli S. 2000. Phagocytic up take of
540 *Encephalitozoon cuniculi* by non professional phagocytes. Infect Immun 68:6939–6945.
541 51. Franzen C, Muller A, Hartmann P, Salzberger B. 2005.Cell invasion and intracellular fate of
542 *Encephalitozoon cuniculi* (Microsporidia). Parasitol 130:285–292.
543 52. Cossart P, Sansonetti PJ. 2004. Bacterial invasion: the paradigms of entero invasive pathogens.
544 Science 304:242–248.
545 53. Guy-Grand D, Griscelli C, Vassali P. 1978. The mouse gut T lymphocyte, a novel type of T
546 cell: nature, origin, and traffic in mice in normal and graft-versus-host conditions. J Exp Med
547 148:1661–1677.
548

549 **Figure legends**

550 Figure 1. a) Photomicrograph of lymphoplasmacytic enteritis in the small intestine (arrowhead) in
551 *Infected* mice. b) Ulceration (arrow) of intestinal mucosa of *Cy-Infected* mice. c) Clusters of *E.*
552 *intestinalis* (arrow) at the glandular region in the mucosa of the ileum of *Cy-Infected* mice. d)
553 Spores counting in the *Infected* and *Cy-Infected* mice. HE staining. ANOVA test with Tukey's
554 posttest showed $p < 0.01$** and $p < 0.001$***.
555

556 Figure 2. Evaluation of T and B cell population in the intestinal mucosa of the mice infected with *E.*
557 *intestinalis* and treated or not with Cy at 7, 14, 21 and 28 dpi. Percentage of lymphocytes CD8 T
558 ($CD19^{-}$ $CD4^{-}CD8^{+}$), CD4 T ($CD19^{-}$ $CD8^{-}$ $CD4^{+}$), NKT cells ($CD19^{-}$ $CD4^{+}$ $NK1.1^{+}$), B-1 ($CD23^{-}$
559 $CD19^{+}$) and B-2 cells ($CD23^{+}$ $CD19^{+}$). ANOVA test with Tukey's post-test showed $p < 0.05$*, p
560 < 0.01** and $p < 0.001$*** compared to non-infected controls.
561

562 Figure 3. Peyer's patch analyzed of the mice infected with *E. intestinalis* and treated or not with Cy
563 for 7, 14, 21 and 28 dpi. a) Percentage of dendritic cells ($CD11c^{+}$) in Peyer's Patch. b)
564 Photomicrograph of Peyer's Patch with lymphoid expansion in *Infected* group or rarified lymphoid

bioRxiv preprint doi: https://doi.org/10.1101/611988; this version posted April 22, 2019. The copyright holder for this preprint (which was not certified by peer review) is the author/funder. All rights reserved. No reuse allowed without permission.

565 tissue in *Cy-Infected* group. HE staining. ANOVA test with Tukey's post-test showed p <0.05*,

566 <0.01** and <0.001*** compared to non-infected controls.

567

568 Figure 4. Cell population in the mesenteric lymph nodes of the mice infected with *E. intestinalis*

569 and treated or not with Cy for 7, 14, 21 and 28 dpi. Percentage of B-2 cells ($CD23^{+}$ $CD19^{+}$),

570 macrophages ($CD19^{-}$ $CD11b^{+}$), CD4 T cells ($CD19^{-}$ $CD8^{-}$ $CD4^{+}$), CD8 T cells ($CD19^{-}$ $CD4^{-}$ $CD8^{+}$)

571 and NKT cells ($CD19^{-}$ $CD4^{+}$ $NK1.1^{+}$). ANOVA test with Tukey's post-test showed p <0.05* and p

572 <0.01**.

573

574 Figure 5. T and B population in the peritoneum of the mice infected with *E. intestinalis* and treated

575 or not with Cy for 7, 14, 21 and 28 dpi. The number of CD8 T cells ($CD19^{-}$ $CD4^{-}$ $CD8^{+}$), CD4 T

576 cells ($CD19^{-}$ $CD8^{-}$ $CD4^{+}$), NKT cells ($CD19^{-}$ $CD4^{+}$ $NK1.1^{+}$), B-1 cells ($CD23^{-}$ $CD19^{+}$), B-2

577 ($CD23^{+}$ $CD19^{+}$) cells, and macrophages ($CD19^{-}$ $CD11b^{+}$). ANOVA test with Tukey's post-test

578 showed p <0.05*, p <0.01** and p <0.001*** compared to non-infected controls.

579

580 Figure 6. Proinflammatory cytokines (IL-2, IL-6, IFN-γ, and TNF-α) and anti-inflammatory

581 cytokines (IL-4, IL-10, and IL-17A) levels in the intestine of mice infected with *E. intestinalis* and

582 treated or not with Cy for 7, 14, 21, and 28 dpi. ANOVA test with Tukey's posttest.

583

584 Figure 7. TEM from the intestine of *Cy-Infected* mice. a, b, and c*) E. intestinalis* spores adhered to

585 and enterocyte (*). Note that microvillosities disappeared, the membrane shows invaginations

586 associated with an electrodense area in the cytoplasm close to the spore (*). d) Injection of the

587 sporoplasm with loss of microvillosities (arrow). Projections of cytoplasmic membrane involving

588 the extruded polar tubule (arrow).

589

590

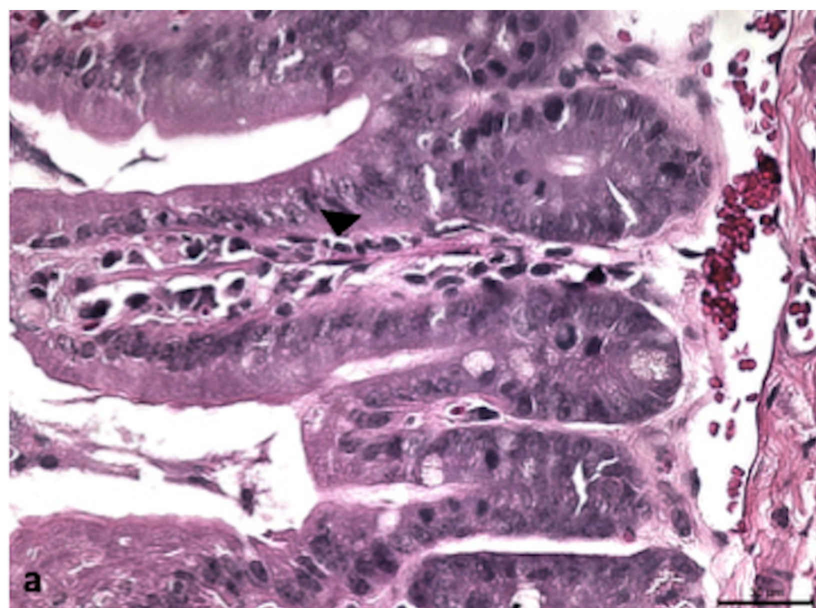
a

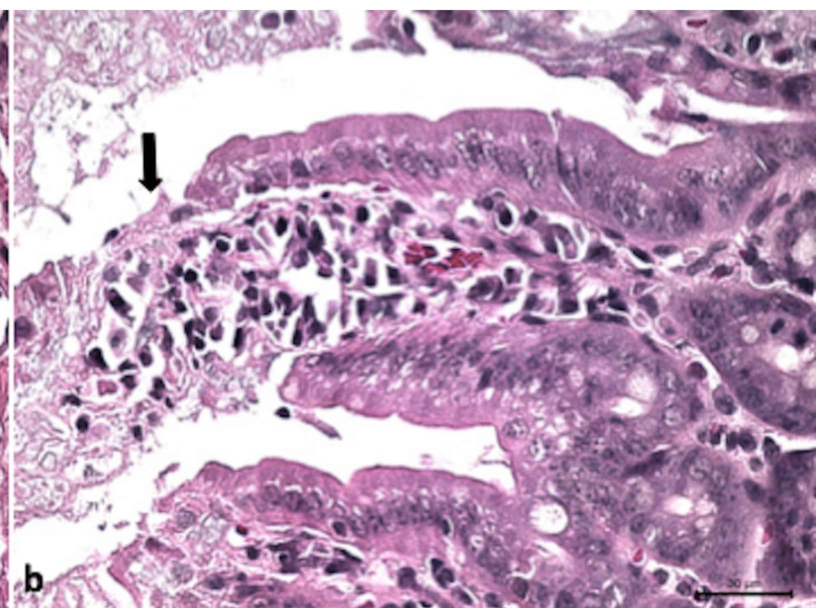
b

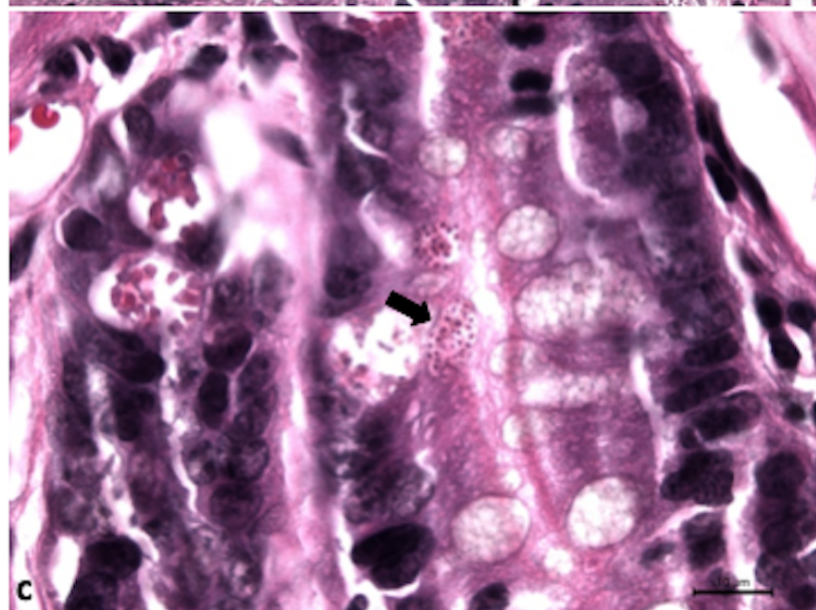
c

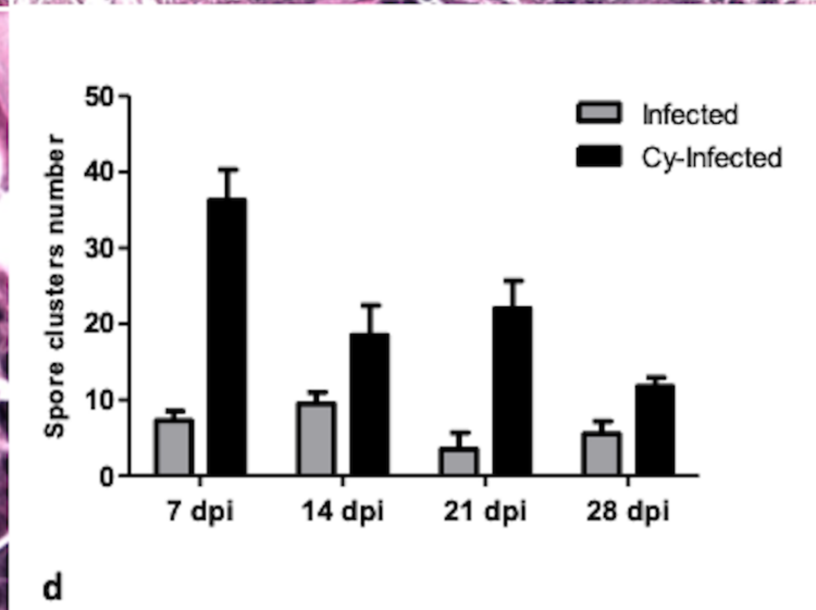
50
40
30
20
10
0
Spore clusters number
Infected
Cy-Infected
7 dpi
14 dpi
21 dpi
28 dpi
d

Intestine

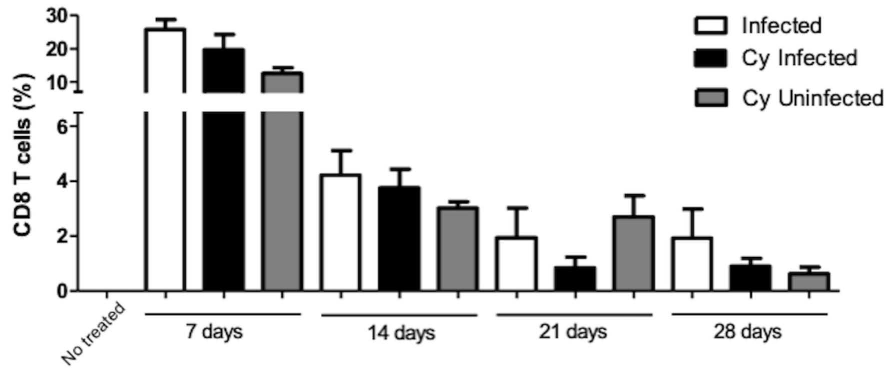

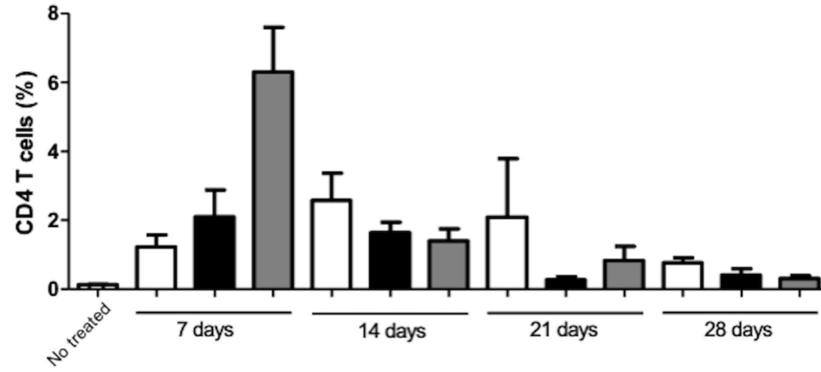

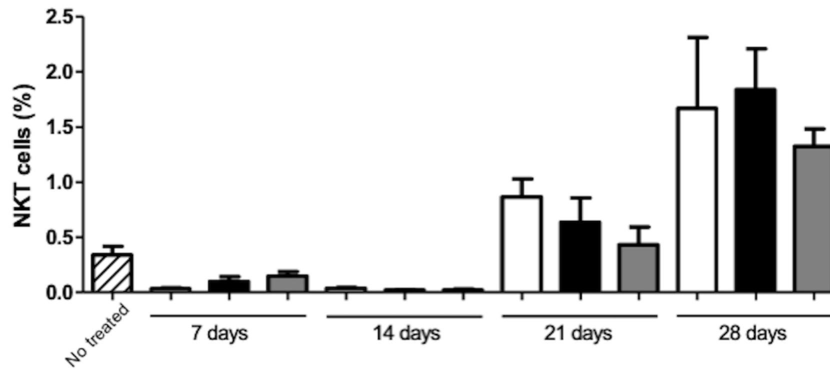

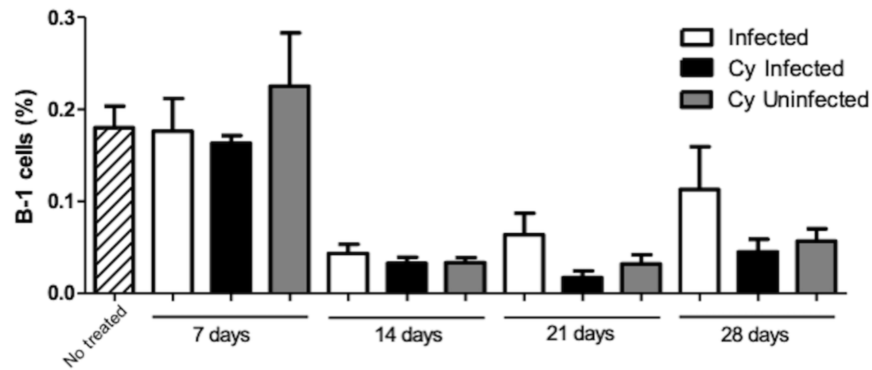

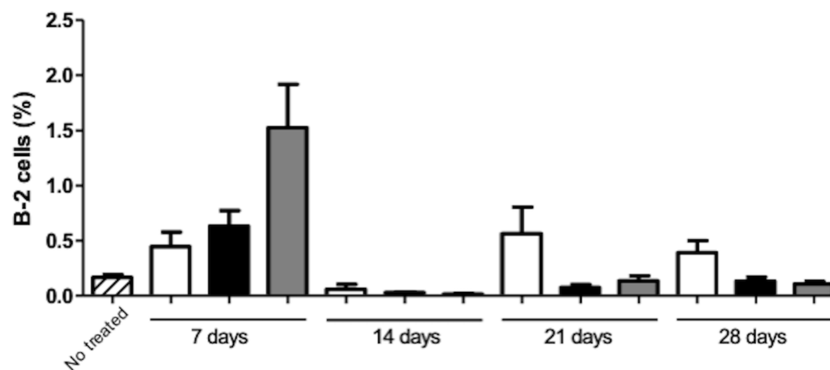

Peyer's patch

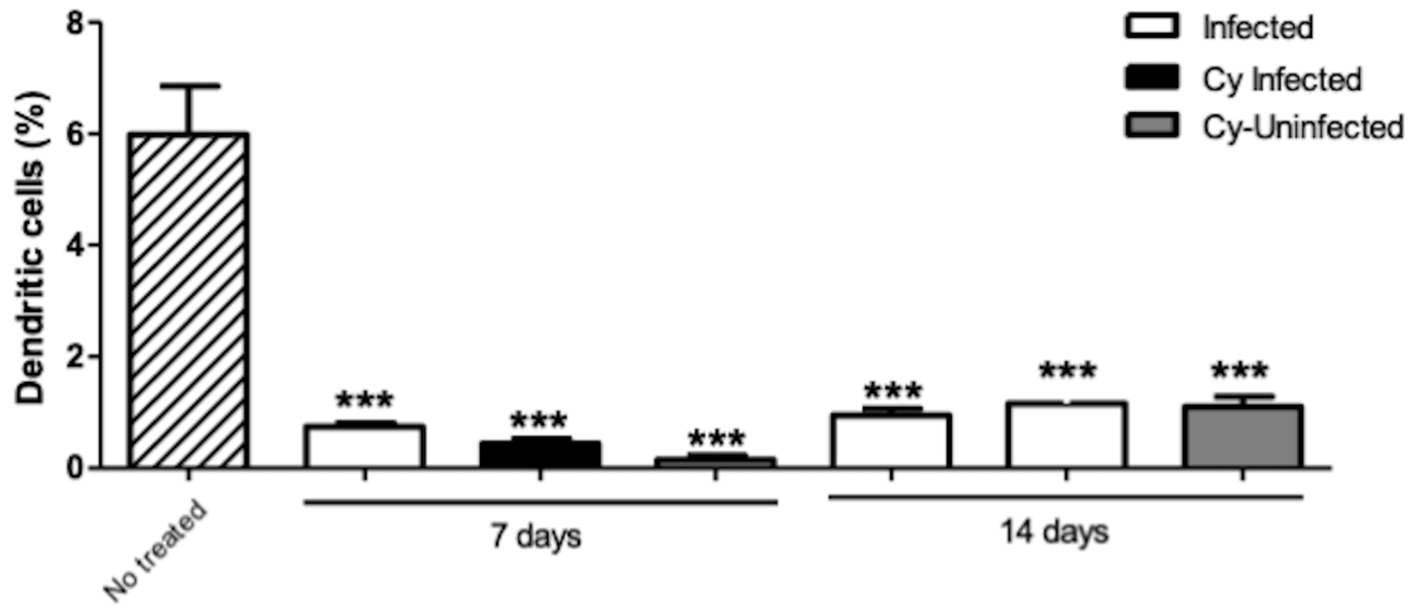

b

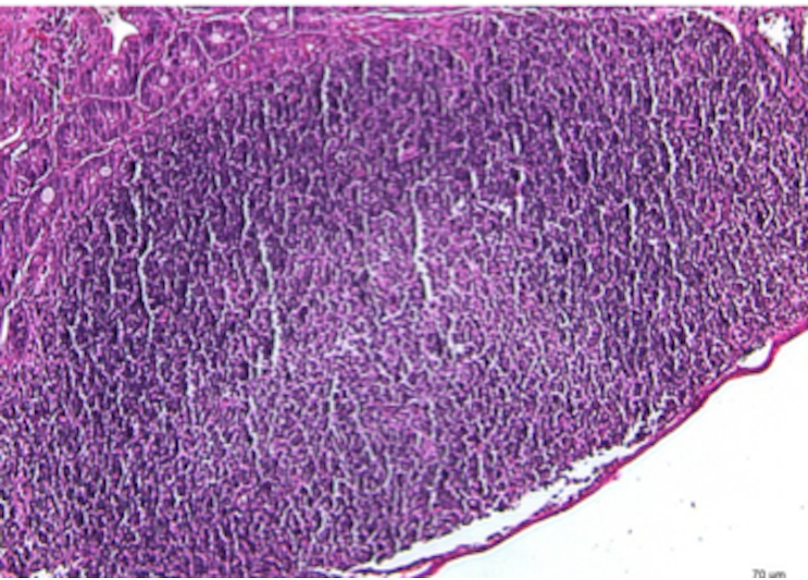

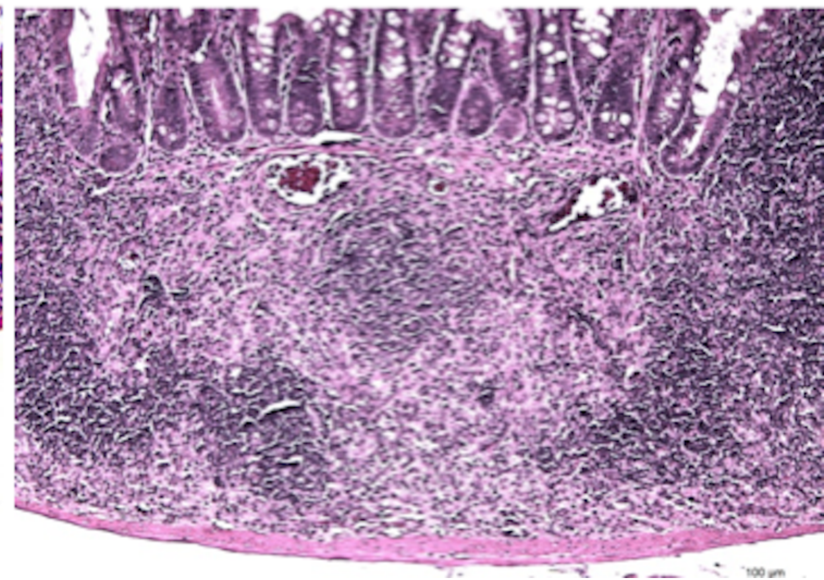

Mesenteric lymph nodes

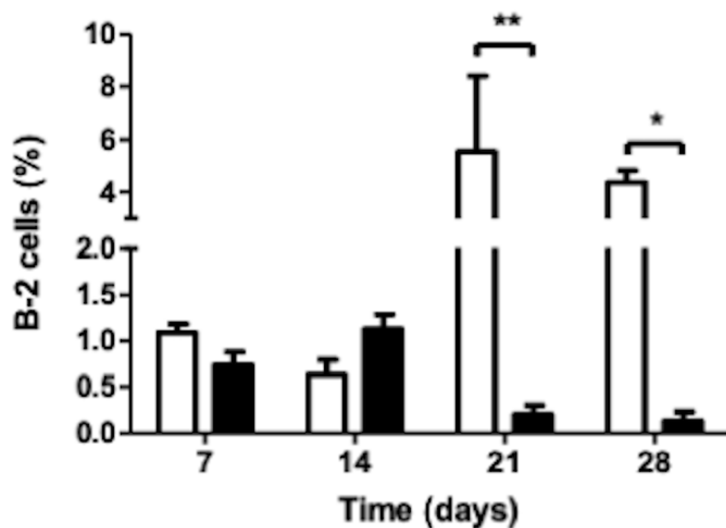

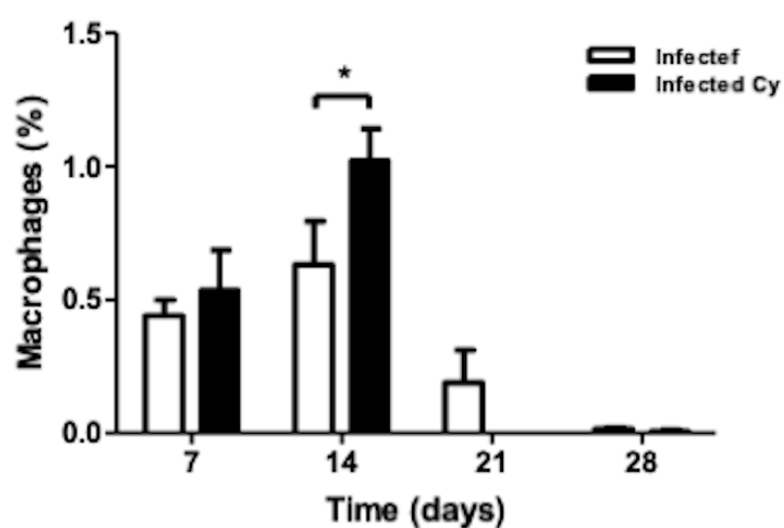

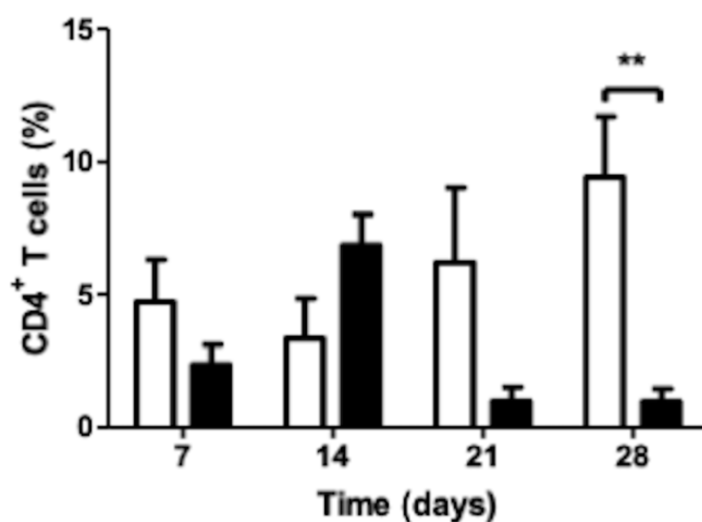

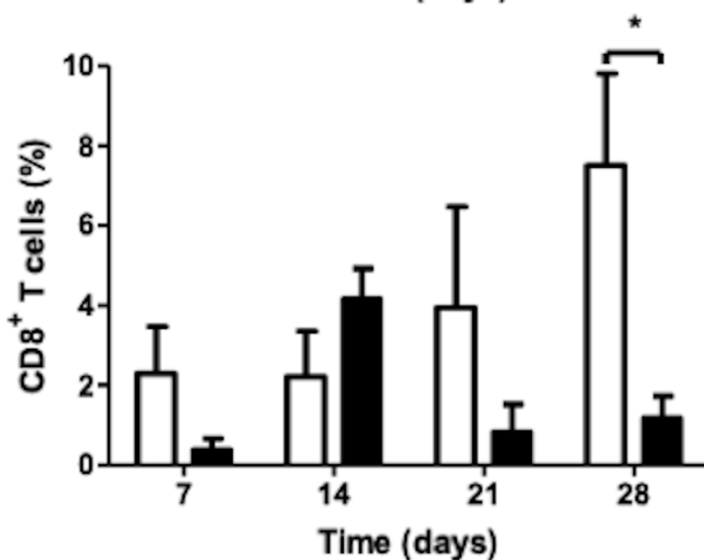

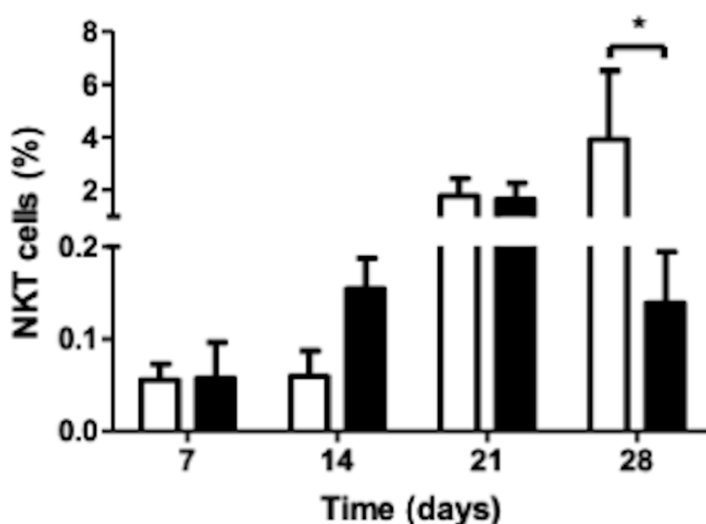

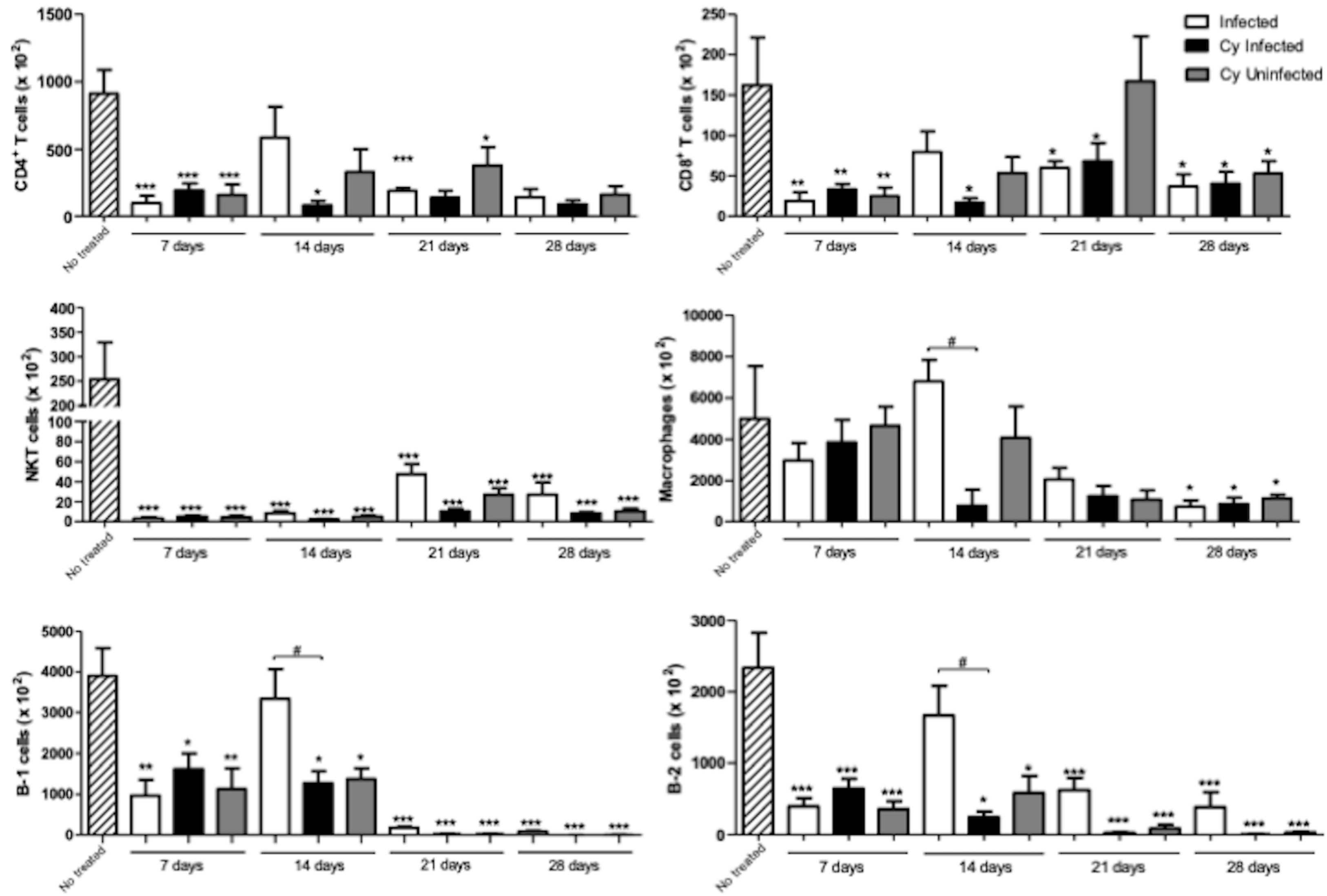
Peritoneum
Infected
Cy Infected
Cy Uninfected
CD4+ T cells (x 10²)
CD8+ T cells (x 10²)
NKT cells (x 10²)
Macrophages (x 10²)
B-1 cells (x 10²)
B-2 cells (x 10²)
No treated
7 days
14 days
21 days
28 days

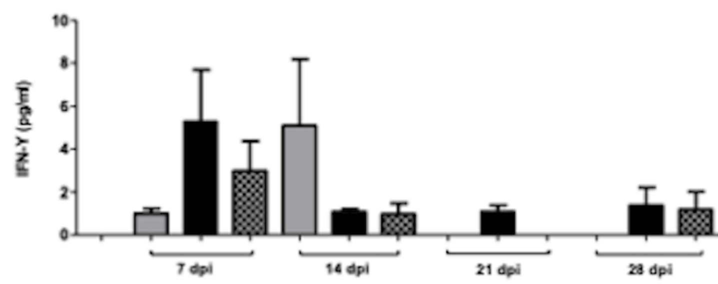
IFN-Y (pg/ml)
10
8
6
4
2
0
7 dpi
14 dpi
21 dpi
28 dpi

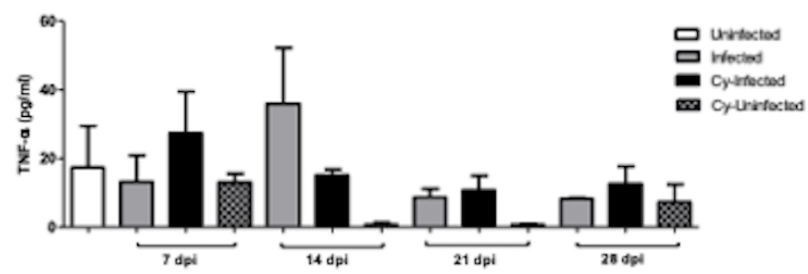
TNF-α (pg/ml)
60
40
20
0
7 dpi
14 dpi
21 dpi
28 dpi
Uninfected
Infected
Cy-Infected
Cy-Uninfected

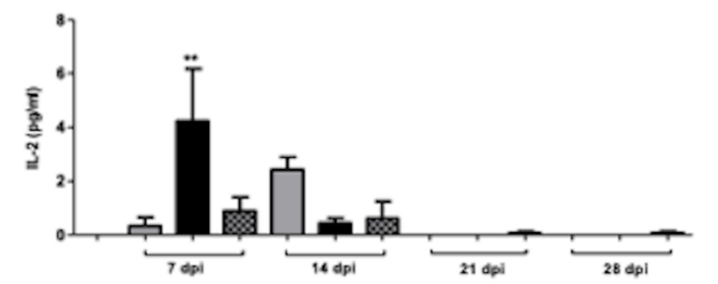
IL-2 (pg/ml)
8
6
4
2
0
**
7 dpi
14 dpi
21 dpi
28 dpi

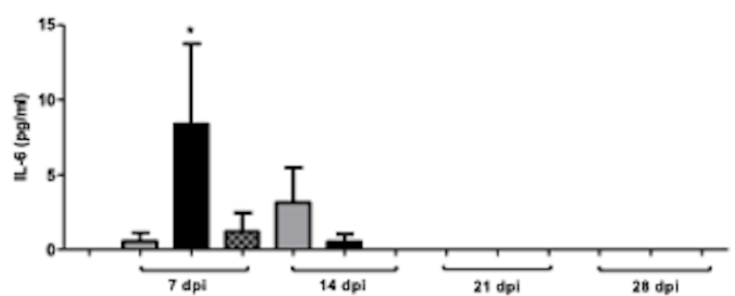
IL-6 (pg/ml)
15
10
5
0
*
7 dpi
14 dpi
21 dpi
28 dpi

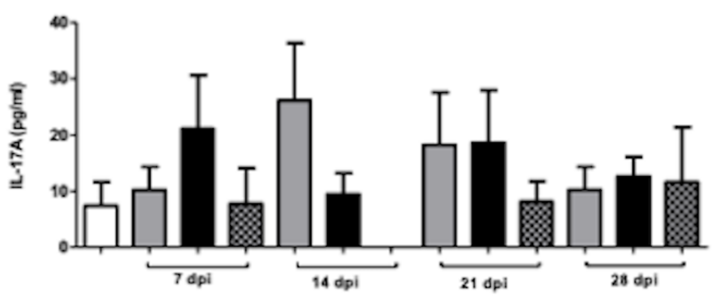
IL-17A (pg/ml)
40
30
20
10
0
7 dpi
14 dpi
21 dpi
28 dpi

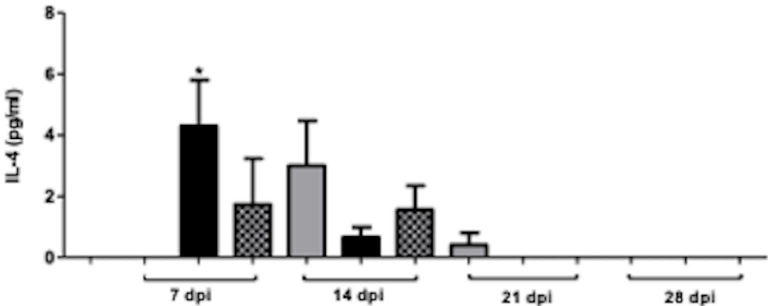
IL-4 (pg/ml)
8
6
4
2
0
*
7 dpi
14 dpi
21 dpi
28 dpi

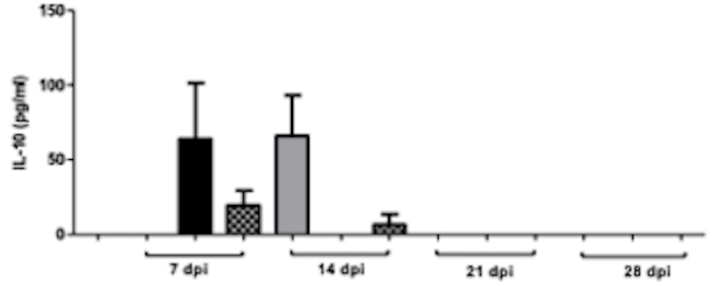
IL-10 (pg/ml)
150
100
50
0
7 dpi
14 dpi
21 dpi
28 dpi

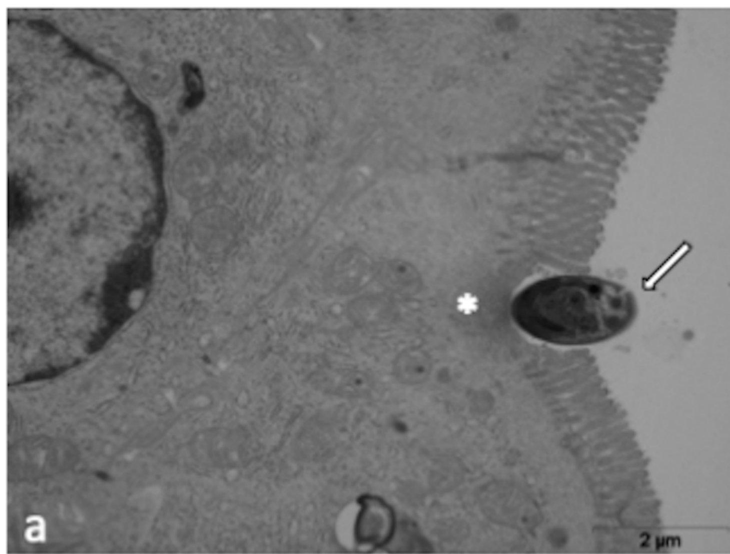
a
2 µm
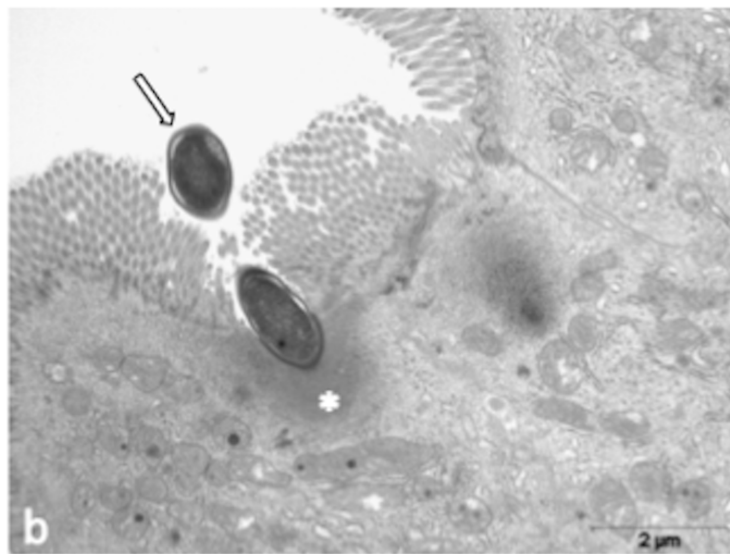
b
2 µm
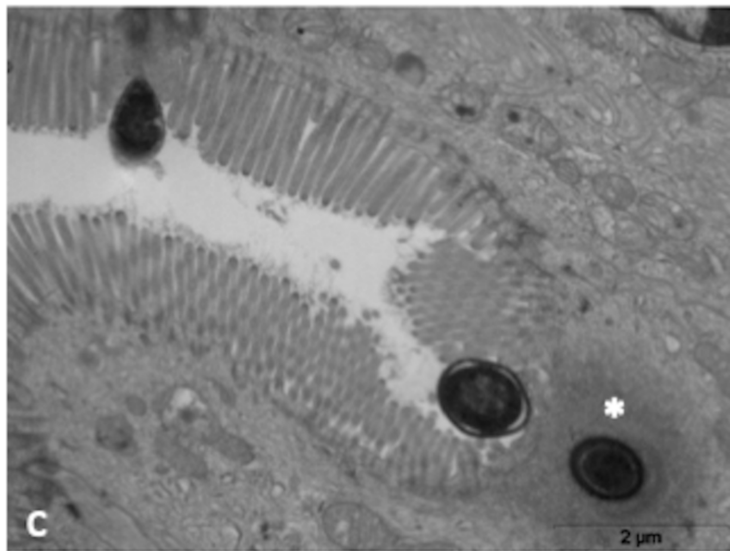
c
2 µm
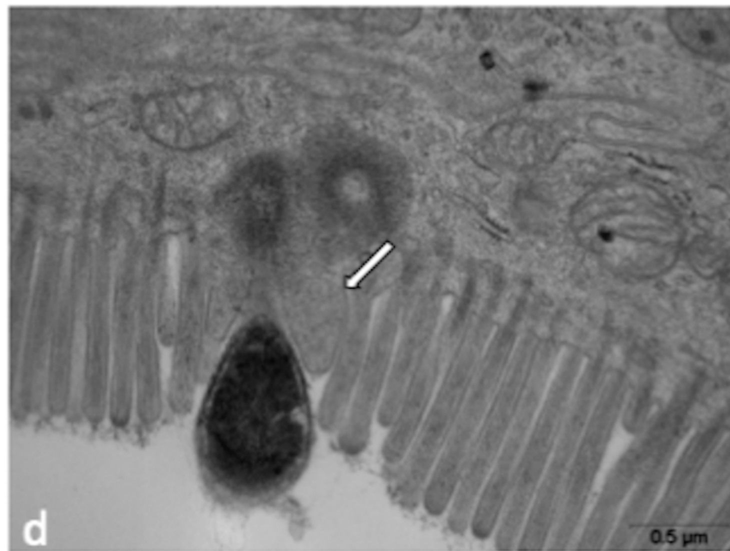
d
0.5 µm